Physics Letters B 679 (2009) 317–320

Contents lists available at ScienceDirect

Physics Letters B

www.elsevier.com/locate/physletb

New experimental limit on photon hidden-sector paraphoton mixing

A. Afanasev [a], O.K. Baker [b,*], K.B. Beard [c], G. Biallas [d], J. Boyce [d], M. Minarni [e], R. Ramdon [a], M. Shinn [d], P. Slocum [b]

[a] Department of Physics, Hampton University, Hampton, VA 23668, USA
[b] Department of Physics, Yale University, PO Box 208120, New Haven, CT 06520, USA
[c] Muons, Inc., 552 N. Batavia Avenue, Batavia, IL 60510, USA
[d] Free Electron Laser Division, Jefferson Laboratory, 12000 Jefferson Avenue, Newport News, VA 23606, USA
[e] Department of Physics, Universitas Riau (UNRI), Pekanbaru, Riau 28293, Indonesia

ARTICLE INFO

Article history:
Received 23 October 2008
Received in revised form 5 April 2009
Accepted 14 July 2009
Available online 28 July 2009
Editor: H. Weerts

PACS:
11.30.Ly
12.20.Fv
12.60.Cn
12.90.+b
13.40.Hq

ABSTRACT

We report on the first results of a search for optical-wavelength photons mixing with hypothetical hidden-sector paraphotons in the mass range between 10^{-5} and 10^{-2} electron volts for a mixing parameter greater than 10^{-7}. This was a generation-regeneration experiment using the "light shining through a wall" technique in which regenerated photons are searched for downstream of an optical barrier that separates it from an upstream generation region. The new limits presented here are the most stringent limits to date on the mixing parameter. The present results indicate no evidence for photon-paraphoton mixing for the range of parameters investigated.

1. Introduction

The Standard Model (SM) of particle physics [1–5] provides a wonderfully successful, well-tested description of the strong, electromagnetic, and weak interactions between half-integer spin fermions and integer spin bosons at the smallest length scales and highest energies accessible in current experiments. However, it has limitations: the apparent failure to explain dark energy and dark matter, an unnaturally small CP-violating parameter associated with the strong interaction, and 19 free parameters, to name a few. If the SM is part of a more fundamental theory which has some new mass scale, new dynamics and particles could appear and hence signal the new physics associated with it. Popular extensions of the SM based upon string theory for example, predict a "hidden sector" of particles that interact with the "visible sector" SM fields only with feeble, gravitational-strength couplings [6,7]. This hidden sector can be probed using very high energy accelerators such as the Large Hadron Collider at the TeV scale, and also by laser experiments at the sub-electron volt (sub-eV) energy scale [8–20]. The importance of this study goes beyond even particle physics. A recent suggestion that paraphotons may give rise to a hidden cosmic microwave background (HCMB) [21] indicates that sub-eV particle physics may have direct bearing on cosmological studies. If there is photon–paraphoton resonant kinetic mixing, then a measurement of this mixing may provide new constraints on the effective number of neutrinos produced after nucleosynthesis and before CMB decoupling [21].

In this hypothesis, low energy dynamics involves the familiar massless electromagnetic force mediator photon, and additionally a hidden sector paraphoton which may have a finite mass. The most general renormalizable Lagrangian describing the interaction dynamics of these two fields at low energies is [6]

$$L = -\frac{1}{4}F^{\mu\nu}F_{\mu\nu} - \frac{1}{4}B^{\mu\nu}B_{\mu\nu} - \frac{1}{2}\chi F^{\mu\nu}B_{\mu\nu} + \frac{1}{2}m_{\gamma'}^2 B_\mu B^\mu. \quad (1)$$

Here $F_{\mu\nu}$ is the ordinary electromagnetic gauge field strength tensor, $B^{\mu\nu}$ is the field strength tensor for the hidden sector field B^μ and $m_{\gamma'}$ denotes the hidden sector paraphoton mass. The first two terms in (1) are the kinetic terms for the SM photon and hidden sector photon fields, respectively. The third term corresponds to a non-diagonal kinetic term, that is, kinetic mixing between the two fields. The last term of the Lagrangian indicates a possible mass for the paraphoton. The mixing parameter χ is predicted to range between 10^{-16} and 10^{-4} in some string theory based calculations [6,7]. However, it is a completely arbitrary parameter and even

* Corresponding author.
E-mail address: oliver.baker@yale.edu (O.K. Baker).

0370-2693
doi:10.1016/j.physletb.2009.07.055

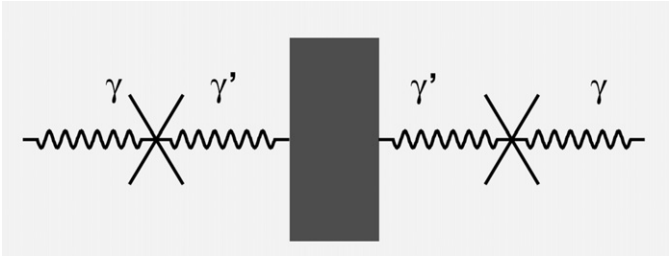

Fig. 1. Photons (γ) may convert into hidden-sector paraphotons (γ') which proceed unimpeded through an optical barrier, reconvert back into photons downstream of the wall, and be detected in a properly executed experiment. The reconverted photons are expected to have the same properties as the original photons in this "light shining through a wall" experiment.

$\chi = 0$ is possible. New limits are placed on this parameter in the work described here.

During the past couple of years, several experimental groups have obtained new data that may illuminate the hidden sector with its potentially small mixing with SM fields in the sub-eV energy range: GammeV [22], BMV [23], OSQAR [24], and PVLAS [25]. These first three experiments are all based upon the "light shining through a wall" technique [12,26] where laser light impinges upon a wall that it cannot penetrate, and a search is made for photons that reappear behind the wall. Only the weakly interacting, small mass, new particle could penetrate the wall and give rise to a regenerated photon signal. Vacuum oscillations of photons (γ) into hidden-sector paraphotons (γ') with sub-eV mass may yield non-vanishing regeneration rates in a carefully designed experiment if such particles exist [6]. The process is depicted in Fig. 1.

2. Experimental procedure

The Light Pseudoscalar and Scalar Search (LIPSS) Collaboration took data that tests the γ–γ' mixing in a series of runs at the Jefferson Lab (JLab) Free Electron Laser (FEL) facility in Spring 2007. The experimental setup is shown in Fig. 2 and is described in more detail, along with the experimental procedure, in [27]. A description is given here that is relevant for the hidden sector photon physics experimental study.

The FEL provided laser light for the LIPSS Experiment that was tuned to a wavelength of 0.935 ± 0.010 microns in pulses that were 150 fs long with a variable repetition rate of up to 75 MHz. The average intensity, monitored continuously during the experiment with a water-cooled power meter as shown in Fig. 2, was 180 watts.

The FEL beam passed through an optical transport system, was collimated to 8 mm beam diameter and was directed onto the LIPSS beam line through a series of water-cooled turning mirrors (TMs) and collimators, as shown in Fig. 2. The LIPSS beam line consisted of an upstream (generation) region between TM2 and TM3 and a separate (regeneration) region from the regeneration region vacuum flange to TM4 downstream of it as indicated. The generation region was 2.9 ± 0.01 meters long; the downstream regeneration region was identical to it. Turning mirror TM3 and the beam dump in combination with a stainless steel vacuum flange on the input to the downstream beam line blocked all incident FEL light from the regeneration region. Any regenerated photons could be detected in the detector system housed in the Light Tight Box (LTB) at the end of the regeneration region. (The experimental setup, as described in [27] included magnetic fields in the generation and regeneration regions. However, that is not relevant here since these present results for paraphoton generation and photon regeneration are independent of magnetic field.)

The LTB was an aluminum case painted on both inner and outer surfaces with black paint, and housed inside a second box of black tape-covered aluminum foil. Inside the Light Tight Box, the photon beam passed a Newport KPX082AR16, 50.2 mm lens which served to focus the photon beam to the desired accuracy onto a CCD array; the array was situated five cm downstream of the lens. The camera system was a Princeton Instruments Spec-10:400BR. It consisted of a back-illuminated CCD with a 1340×400 pixels imaging area (a single pixel is 20 μm × 20 μm in area). Data were recorded to disk using a PC.

The data acquisition system featured onboard grouping (binning) of pixels, where groups of adjacent pixels could be summed before readout to decrease noise. The detection system also consisted of a light emitting diode (LED) and a convex lens used to provide a beam spot on the CCD; this served as a reference spot on the CCD. The calibration of the CCD at the wavelength of FEL light used and at the minimum temperature (−120 °C) was performed using a commercial calibrated source. This was compared with the manufacturer's quoted value for quantum efficiency and CCD well depth [28] and found to be in agreement within experimental error. Note that any regenerated photons have the same properties as the original photons and can be focused to a small spot at the detector. Pointing stability (the direction of the laser beam relative to the central axis of the beam line) was monitored continuously during each data run. The beam was focused onto the pixel array during experimental setup. It was demonstrated in the experiment that the FEL beam was focused to a spot size less than the diameter of a single pixel. The positions of the beam at TM2 and TM3 were monitored continuously during the data runs by cameras and Spiricon LBA-PC software. It was determined that the beam wandered by at most one cm over the length of the beam line. This was due to a combination of transverse motion where the laser beam remained parallel to the beam line axis, and angular deviation with respect to the beamline axis. It is only the latter that results in displacement at the CCD array. An alignment laser (0.5435 nm; less than one watt of power) was used to test this effect, Additionally, the FEL laser light produced at the same wavelength as used in the data runs, but with power levels reduced by many orders of magnitude, was used to test this effect. Laser beam positions at the TMs were correlated with the beam spot at the CCD array in tests performed subsequent to the data run. These tests indicated that the laser light focused onto a single CCD pixel was translated horizontally and vertically by at most the width of a single pixel (20 μm) when the beam position at the TMs was varied by the amount monitored during the data runs. Thus, the signal region for the pixel array was taken to be a 3×3 pixel area at the lens focus; the 3×3 pixel area defined as the signal region did not change during the data runs.

Background contributions to the signal region were studied extensively in the LIPSS setup. Data were collected over a several hour period with the FEL off and with the CCD shutter both open and closed in order to characterize the contributions to background due to stray light leaking into the regeneration region of the beam line. This contribution was measured to be less than a single count per pixel per hour. Data were collected over a period of several hours with the FEL electron beam on but no lasing while the CCD shutter was both open and closed; no difference in count rate was observed. Stray light from fluorescence in gas in the vacuum pipe due to cosmic rays (CRs) was shown to be negligible since the experiment was run with 10^{-6} Torr vacuum in the beam pipes. The readout noise was shown to be 2.5 ± 0.2 counts per pixel per readout. This contribution was minimized by collecting data for at least two hours in each run. CRs that strike the pixel array directly leave clear ionization signals in the pixels that they strike and are easily subtracted from the data. Runs that contain a CR muon hit on any

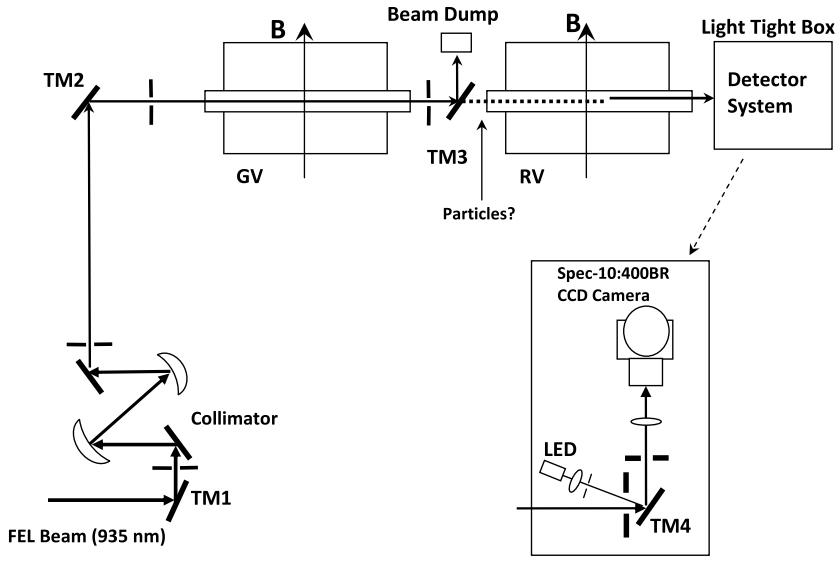

Fig. 2. The LIPSS experimental setup. Laser light from the JLab FEL is directed onto the LIPSS beamline via TM1 and a collimator. TM2 directs the properly prepared laser beam onto the generation region upstream of the beam dump at TM3. No incident photons pass through the beam dump. An identical regeneration region sits downstream of the optical barrier. Paraphotons could pass through the wall and be reconverted into photons which are then detected in the LTB.

pixel within an area of 100×100 pixels around the signal region were discarded. The camera system was cryogenically cooled to $-120\,^{\circ}$C resulting in the lowest dark current that can be achieved under these experimental conditions; less than one single count per pixel per hour. This was also verified experimentally. A check for long term drifts of the pixel thermal noise showed that this contribution was negligible over a period of several days [28].

The data were analyzed by defining a signal region where any regenerated photons could be observed, and background regions where no signal was expected. Light from a green (0.5435 microns) laser placed upstream of TM1 was focused onto the CCD array through the focusing lens shown in Fig. 2. Then, the FEL was placed in the so-called alignment mode where the laser average power was reduced by several orders of magnitude (to 0.05 percent duty factor) so as not to damage the CCD optics and aligned in precisely the same way and focused onto the array. The lower duty factor was rigorously maintained for both machine and personnel safety when in alignment mode. In both cases, it was demonstrated that the laser light was focused by the lens down to the same, single pixel. Alignment mode runs were taken before and after the data runs, and were interspersed during the data runs in order to check for long term beam motion. No such effect was observed over the running period.

The nine pixels in the signal area were binned together in software for each run. All other pixels and pixel groupings outside the signal region were used to define the background region(s). The difference between the counts in the signal region and the counts in the background region (normalized to the number of pixels in the signal region) was determined for all data runs. No excess events above background were seen in any single run, or if all runs were combined. Twenty hours of data were taken and analyzed corresponding to a total accumulated photon count of 6.1×10^{25} photons.

3. Results

The rate of regenerated photons, r_s, is given by

$$r_s = r_i P_{\text{trans}} \frac{\Delta\Omega}{\Omega} \varepsilon, \tag{2}$$

where r_i is the FEL (incident) photon rate, $\Delta\Omega/\Omega$ is the photon collection efficiency (solid angle for detection) determined to be 94%, ε is the detector quantum efficiency which was 40% at the wavelength used in the data runs, and [6]

$$P_{\text{trans}} = 16\chi^4 \left[\sin\left(\frac{\Delta k L_1}{2}\right) \sin\left(\frac{\Delta k L_2}{2}\right) \right]^2 \tag{3}$$

is the probability for photon regeneration from paraphotons that mix with incident photons in the generation region and propagate through the wall indicated in Fig. 1. Here χ is the mixing parameter defined in (1), L_1 (L_2) is the length of the generation (regeneration) region shown in Fig. 2 and the momentum difference between the photon and the hidden-sector paraphoton is defined as

$$\Delta k = \omega - \sqrt{\omega^2 - m_{\gamma'}^2} \approx \frac{m_{\gamma'}^2}{2\omega} \quad (\text{for } m_{\gamma'} \ll \omega) \tag{4}$$

where ω is the laser photon energy (1.33 eV) and $m_{\gamma'}$ is the paraphoton mass.

The background rate is determined by comparison of the following two procedures. In one case, the number of counts in the nine-pixel signal region is determined when there is no laser light in the beam line. In the second approach, the rate in the large number of pixels in the CCD array that are outside of the signal region is determined, in order to get a large number of statistics. This number is then normalized to a nine pixel signal region. The result is the same in both approaches. There is no indication of an excess of events above background for any cuts applied to the data.

The Significance of the result is defined as $n_s/\sqrt{n_b}$, where n_s is the number of events in the signal region as described above and n_b is the number of events in the pixels used as background measurements. From this Significance, a 99% Confidence Limit is calculated.

The results from this experiment can therefore be used to set the new limits on the mixing χ of photons to hypothetical hidden-sector paraphotons that are shown in Fig. 3. Making use of the values given above for generation and regeneration lengths, photon energy and incident rates, efficiencies and solid angles, and using (2) and (3) the maximum value for P_{trans} in this experi-

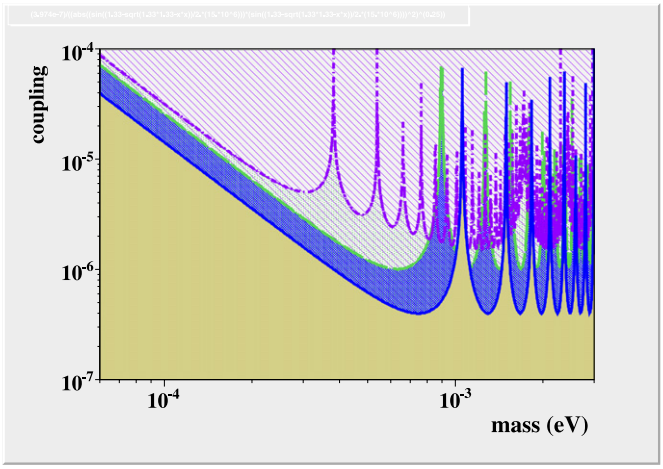

Fig. 3. A mixing parameter χ versus hidden sector paraphoton mass. Upper limits (95% confidence) set by the recent "light shining through wall" experiments [6]. The purple (upper) curve is from the BMV Collaboration [23], the green (middle) curve is from the GammeV Collaboration [22], and the blue curve is the new result from the LIPSS Collaboration (99%). The different structures for the curves correspond to the different photon energies and baselines used in the different experiments.

ment is 1.57×10^{-24}. This result also makes use of the measured background rate of 2.29×10^{-3} Hz for the group of nine pixels in the signal region, accumulated for 20 hours. The blue curve is the new LIPSS result, compared with those from the GammeV [22] and BMV [23] collaborations. The region above the curves is ruled out in each case. This LIPSS result represents the most stringent limits to date on this mixing in a generation–regeneration experiment in this range of parameters. The limits set by the BFRT Collaboration [29] are less than those presented in Fig. 3 for each case.

Acknowledgements

The authors thank the technical staff of the Jefferson Lab Free Electron Laser Facility, especially F. Dylla, G. Neil, G. Williams, R. Walker, D. Douglas, S. Benson, K. Jordan, C. Hernandez-Garcia, and J. Gubeli, as well as M.C. Long of Hampton University for their excellent support of the experimental program. Funding from the Office of Naval Research Award N00014-06-1-1168 is gratefully acknowledged.

References

[1] S. Glashow, Nucl. Phys. 22 (1961) 579.
[2] S. Weinberg, Phys. Rev. Lett. 19 (1967) 1264.
[3] A. Salam, in: W. Swatholm (Ed.), Elementary Particle Theory, Almquist and Wiksell, Stocholm, 1968.
[4] H.D. Politzer, Phys. Rev. Lett. 30 (1973) 1346.
[5] D. Gross, F. Wilczek, Phys. Rev. Lett. 30 (1973) 1343.
[6] M. Ahlers, et al., Phys. Rev. D 77 (2008) 095001.
[7] J. Jaeckel, A. Ringwald, Phys. Lett. B 659 (2008) 509.
[8] B. Holdom, Phys. Lett. B 166 (1986) 196.
[9] R. Foot, X.G. He, Phys. Lett. B 267 (1991) 509.
[10] K.R. Dienes, et al., Nucl. Phys. B 492 (1997) 104.
[11] S.A. Abel, B.W. Schofield, Nucl. Phys. B 685 (2004) 150.
[12] L.B. Okun, Sov. Phys. JETP 56 (1982) 502.
[13] V.V. Popov, O.V. Vasil'ev, Europhys. Lett. 15 (1991) 7.
[14] M. Ahlers, et al., Phys. Rev. D 75 (2007) 035011.
[15] A. Ringwald, J. Phys. Conf. Ser. 39 (2006) 197.
[16] J. Khoury, A. Weltman, Phys. Rev. Lett. 93 (2004) 171104.
[17] J. Khoury, A. Weltman, Phys. Rev. D 69 (2004) 044026.
[18] D.F. Mota, D. J Shaw, Phys. Rev. D 75 (2007) 063501.
[19] D.F. Mota, D.J. Shaw, Phys. Rev. Lett. 97 (2006) 151102.
[20] G. Raffelt, W.-M. Yao, et al., Particle Data Group, J. Phys. G 33 (2006) 1.
[21] J. Jaeckel, J. Redondo, A. Ringwald, Phys. Rev. Lett. 101 (2008) 131801, arXiv:0804.4157v1 [astro-ph].
[22] A. Chou, et al., Phys. Rev. Lett. 100 (2008) 080402.
[23] M. Fouche, et al., Phys. Rev. D 78 (2008) 032013;
C. Robilliard, et al., Phys. Rev. Lett. 99 (2007) 190403.
[24] R. Ballou, et al., CERN Report, CERN-SPEC-2007-039 (2007).
[25] E. Zavattini, et al., arXiv:0706.3419 [hep-ex].
[26] K.V. Bibber, et al., Phys. Rev. Lett. 59 (1987) 759.
[27] A. Afanasev, et al., Phys. Rev. Lett. 101 (2008) 120401.
[28] LIPSS Collaboration, 2009, in preparation.
[29] R. Cameron, et al., Phys. Rev. D 47 (1993) 3707.